Observations of the impact of a major Saharan dust storm on the atmospheric radiation balance

A. Slingo,[1] T. P. Ackerman,[2] R. P. Allan,[1] E. I. Kassianov,[2] S. A. McFarlane,[2] G. J. Robinson,[1] J. C. Barnard,[2] M. A. Miller,[3] J. E. Harries,[4] J. E. Russell,[4] and S. Dewitte[5]

Received 14 August 2006; revised 12 October 2006; accepted 10 November 2006; published 30 December 2006.

[1] Saharan dust storms have often been observed from space, but the full impact on the Earth's radiation balance has been difficult to assess, due to limited observations from the surface. We present the first simultaneous observations from space and from a comprehensive new mobile facility in Niamey, Niger, of a major dust storm in March 2006. The results indicate major perturbations to the radiation balance both at the top of the atmosphere and at the surface. Combining the satellite and surface data, we also estimate the impact on the radiation balance of the atmosphere itself. Using independent data from the mobile facility, we derive the optical properties of the dust and input these and other information into two radiation models to simulate the radiative fluxes. We show that the radiation models underestimate the observed absorption of solar radiation in the dusty atmosphere. **Citation:** Slingo, A., et al. (2006), Observations of the impact of a major Saharan dust storm on the atmospheric radiation balance, *Geophys. Res. Lett.*, *33*, L24817, doi:10.1029/2006GL027869.

1. Introduction

[2] Dust storms from the Sahara transport large quantities of material across the African continent and beyond, causing widespread disruption and hazards to health. The dust is frequently deposited into the Atlantic Ocean, where it provides an important source of nutrients [*Mahowald et al.*, 2005], and can be carried as far as the West Indies [*Prospero and Lamb*, 2003]. Such events may also suppress the growth of Atlantic tropical cyclones [*Dunion and Velden*, 2004]. Satellite observations have enabled estimates to be made of the effect of the dust on the radiation balance seen from space [*Kaufman et al.*, 2002], but only limited in situ observations have hitherto been made at the surface [*Washington et al.*, 2006]. In this study, the first simultaneous and continuous observations are presented of the effect of a major dust storm in March 2006 on the radiation balance both at the top of the atmosphere (TOA) and at the surface.

[1]Environmental Systems Science Centre, University of Reading, Reading, UK.
[2]Pacific Northwest National Laboratory, Richland, Washington, USA.
[3]Brookhaven National Laboratory, Atmospheric Science Division, Upton, New York, USA.
[4]Blackett Laboratory, Imperial College London, London, UK.
[5]Royal Meteorological Institute of Belgium, Brussels, Belgium.

0094-8276/06/2006GL027869$05.00

2. Data and Methodology

[3] This study combines data from the Geostationary Earth Radiation Budget (GERB) broadband radiometer [*Harries et al.*, 2005] and the Spinning Enhanced Visible and InfraRed Imager (SEVIRI) on the Meteosat-8 weather satellite [*Schmetz et al.*, 2002] with measurements from a new Mobile Facility located in Niamey, Niger (13° 29′N, 2° 10′E), operated by the US Atmospheric Radiation Measurement (ARM) program [*Ackerman and Stokes*, 2003].

[4] GERB and SEVIRI provide continuous observations with a temporal resolution of 15 minutes. The solar and thermal fluxes in the Edition 1 release of the GERB data [*Harries et al.*, 2005] have a resolution of about 40 km. In this work, we use a resolution enhanced GERB/SEVIRI hybrid product (NRT V003 ARCH product) with a resolution of about 10 km, which uses the GERB climate-quality measurements in its derivation (S. Dewitte et al., The Geostationary Earth Radiation Budget edition 1 data processing algorithms, submitted to *Advances in Space Research*, 2006, hereinafter referred to as Dewitte et al., submitted manuscript, 2006). We also use measurements from the CERES [*Wielicki et al.*, 1996] broadband instruments on the polar-orbiting TERRA and AQUA satellites at the twice-daily overpass times (only for pixels with centres within 0.1 degrees of the GERB/ARCH pixel centre). We used the ES8_Terra-FM1_Edition1-CV_026029 and ES8_Aqua-FM3_Edition1-CV_026029 versions of the CERES data. These data were obtained from the Atmospheric Science Data Center at NASA Langley Research Center.

[5] The ARM Mobile Facility (AMF) includes a wide range of passive and active instruments for measuring the radiative fluxes at the surface and the atmospheric structure above the site. The AMF is currently deployed at Niamey airport for all of 2006 as part of the RADAGAST project [*Miller and Slingo*, 2006] (Radiative Atmospheric Divergence using Arm mobile facility, Gerb data and Amma STations), in cooperation with the African Monsoon Multidisciplinary Analysis (AMMA) experiment [*Lebel et al.*, 2003].

[6] The errors in the radiative fluxes observed by the above platforms are as follows. These estimates are based on the analysis of many years of data obtained at the permanent ARM sites and of the GERB data obtained both during ground calibration and since the launch of the instrument in 2002. GERB measures directional radiances which are converted to hemispheric fluxes by applying angular models. The absolute accuracy of solar radiances is estimated to be 2.25% and of thermal radiances 0.96%. Angular models introduce additional uncertainties, estimated

to be 10 Wm^{-2} for typical solar fluxes and 5 Wm^{-2} for thermal fluxes, although values may be larger for aerosol for which there is no explicit angular model. The radiometers at the ARM Mobile Facility are maintained daily, building on the methodology developed within both the ARM and international programmes [*Ohmura et al.*, 1998]. Best estimates of the operational accuracy of the measurements taken over long periods are as follows. Uncertainties in the downwelling solar fluxes are estimated to be 13.6 Wm^{-2} (direct), 9.0 Wm^{-2} (diffuse) and 9.0 Wm^{-2} (total). However, the uncertainty is likely to be much larger during the very unusual circumstances of the duststorm, when very high diffuse fluxes were observed (700 Wm^{-2}). Following recent work [*Reda et al.*, 2003], we estimate that under these conditions the diffuse uncertainty may be as large as 22 Wm^{-2}. The uncertainty in the downwelling thermal flux is estimated to be 5.1 Wm^{-2}. Assuming uncorrelated errors between GERB and the AMF, uncertainties in the time-averaged solar divergences across the atmosphere shown in section 4 are estimated to be 15 Wm^{-2} (one sigma) at best. Work is ongoing to refine all of these error estimates.

[7] Several AMF instruments provide information on aerosols. In this work, retrievals of the aerosol optical depth and radiative effective radius (R_{eff}) are made from data obtained by the Multi-Filter Rotating Shadowband Radiometer, MFRSR [*Kassianov et al.*, 2005]. The MFRSR measures spectral values of total and diffuse solar irradiances at six wavelengths (0.415, 0.5, 0.615, 0.673, 0.870 and 0.94 μm). These are used to obtain direct solar irradiances which in turn are applied to derive the aerosol optical depth [*Harrison and Michalsky*, 1994]. We derived the aerosol microphysical (e.g., effective radius) and optical (aerosol optical depth, single-scattering albedo and asymmetry parameter) properties from MFRSR observations by using an updated version of the retrieval technique described by *Kassianov et al.* [2005]. The technique requires assumptions regarding the shape of the aerosol size distribution (a combination of two lognormal distributions), the real part of the refractive index, as well as the spectral values of surface albedo. The latter were estimated from MODIS data [*Schaaf et al.*, 2002]. The technique includes two basic steps; the first provides the aerosol size distribution. Parameters of two lognormal distributions are iterated to match the spectral dependence of the aerosol optical depth. The second step estimates the imaginary part of the refractive index. Values of the imaginary refractive index (for a given size distribution) are iterated to match the spectral dependence of the ratio of the diffuse to the direct irradiances, the so-called diffuse-to-direct ratio. The retrieved single scattering albedos at 0.5 μm are in the range 0.89–0.95, compared with 0.95–0.99 at 0.55 μm in a recent aircraft study [*Haywood et al.*, 2003], indicating higher absorption in the retrievals used here. Comparisons with independent aerosol retrievals are planned to investigate these differences. Retrievals were not performed for days with significant amounts of high-level cloud, because cloud also affects the irradiances and makes it impossible to perform the retrievals.

3. Results

[8] The dust storm was initiated on 5 March 2006, when anomalously strong northerly flow produced a wide front of dust in the lee of the Atlas mountains in northern Algeria. The flow propagated southwards across the Sahara over the following days, lifting more dust into the atmosphere. The dust reached Niamey at 0930 local time on 7 March 2006, leading to a reduction in the visibility from 10 km to below 1 km over the next few hours and a drop in the daytime maximum temperature of about 10°C over the next few days. Figure 1a shows a dust diagnostic derived from three of the SEVIRI infrared channels, at about the time of greatest thickness in Niamey. The dust appears pink and is concentrated into several plumes. Animations clearly show the southward movement of the dust, which appeared to propagate close to the surface as a density current, with the flow following the lowest terrain and moving around the highest topography (e.g. the Tibesti) or being channeled through low mountain passes (in the Hoggar and Air massifs). In this respect, the storm behaved similarly to an earlier large outbreak in March 2004 [*Knippertz and Fink*, 2006], although the meteorological conditions in the present event remain to be investigated.

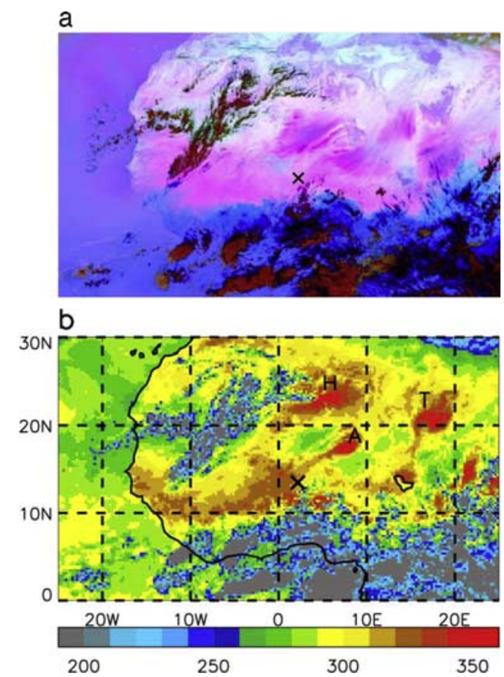

Figure 1. (a) Dust product for 1200 GMT on 8 March 2006, derived from three infrared channels of the SEVIRI imager on Meteosat-8, with centre wavelengths at 12.0, 10.8 and 8.7 μm. This false-color image was created using an algorithm from EUMETSAT, which colors red the difference between the 12.0 and 10.8 μm channels, green the difference between the 10.8 and 8.7 μm channels and blue the 10.8 μm channel. Dust appears pink or magenta, water vapor dark blue, thick high-level clouds red-brown, thin high-level clouds almost black and surface features pale blue or purple. (b) Outgoing Longwave Radiation (Wm^{-2}) derived from the GERB broadband radiometer. The Hoggar (H), Air (A) and Tibesti (T) mountain ranges are indicated. The location of Niamey is marked by a cross on both images.

[9] Figure 1b shows the outgoing longwave radiation (OLR) derived from the GERB and SEVIRI data [*Harries et al.*, 2005; Dewitte et al., submitted manuscript, 2006] at

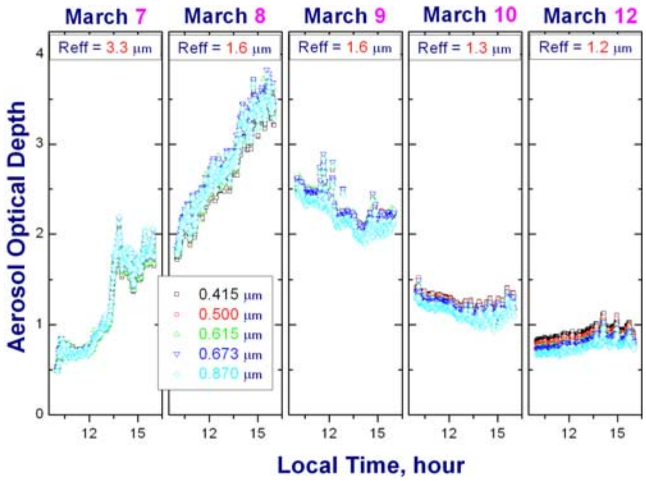

Figure 2. Aerosol optical depth and effective radius at Niamey, at five visible wavelengths. The aerosol optical properties were retrieved from daytime measurements by the Multi-Filter Rotating Shadowband Radiometer (MFRSR) at the Mobile Facility.

the same time as for the top panel. The Hoggar, Air and Tibesti mountain ranges appear red (warm) in this image. Deep minima, appearing blue or grey, are due to clouds, but there are also lesser minima (appearing green) to the south and west of the mountains, that correspond to the densest patches of dust in the upper panel, which reduce the OLR by about 30 Wm^{-2} compared with nearby regions. Comparisons of GERB data from previous years with the Met Office weather forecast model [*Allan et al.*, 2005; *Haywood et al.*, 2005] showed that even larger OLR perturbations are possible in the northern summer, when convection transports the dust to much higher levels.

[10] The MFRSR retrievals in Figure 2 show that the dust arrived at Niamey in two episodes on 7 March, with the second wave bringing the densest aerosol at around 1400 local time. The retrieved effective radius was 3.3 μm at the start of the event and decreased steadily over the following days. The optical depth continued to rise to a peak of 3–4 late on 8 March, dropping thereafter to more typical background levels.

[11] The perturbations to the radiation balance are shown in Figure 3. Unfortunately, GERB data are missing for about two days immediately before the dust event, but are continuous thereafter. Broadband data from the CERES instruments are also shown [*Wielicki et al.*, 1996]. Incoming solar fluxes at the TOA (not shown in Figure 3, but required to calculate the atmospheric absorption) were obtained using the radiation code in the Met Office model [*Pope et al.*, 2000]. The onset of the dust storm had a major impact on the solar radiation balance. At midday, reflected fluxes at the TOA rose by 100 Wm^{-2} while the incoming solar fluxes at the surface dropped by around 250 Wm^{-2}. The resulting solar heating of the atmosphere at midday rose from about 250 Wm^{-2}, or 19% of the incoming solar radiation at the TOA, prior to the dust storm, to over 400 Wm^{-2} (31% of the incoming solar at the TOA) at the height of the dust storm on 8 March.

[12] Thermal fluxes also show large signals from the dust. The OLR falls by about 30 Wm^{-2} at midday, consistent with the perturbations shown in Figure 1b and the analysis of previous dust storms [*Haywood et al.*, 2005]. The surface emission drops by over 100 Wm^{-2}, corresponding to a surface cooling of 13°C. In contrast, the downward thermal emission from the atmosphere shows a significant peak on 7 March, despite the fact that atmospheric temperatures and humidities both drop during the event. To investigate the cause of these changes, we used the formula derived by *Prata* [1996] to estimate the downward thermal emission in clear skies in the absence of dust, using as input the AMF measurements of the surface air temperature and column water vapor. The estimated fluxes are also shown in Figure 3. As expected, these fluxes show a progressive decrease through the event as the atmosphere cools and dries, with no peak on 7 March. The enhanced emission observed on 7 March and thereafter is thus attributable directly to the additional emission from the dust itself. This emission is particularly strong on 7 March, due to the larger particle sizes shown in Figure 2.

[13] The net thermal cooling of the atmosphere (Figure 3f) increases through the event, but the behavior is complicated by the competing signals from the increased atmospheric opacity and the decreased temperature of the surface and lower atmosphere. The increased thermal cooling offsets only a part of the increased solar heating, so the net radiative heating of the atmosphere (not shown) increases by about 100 Wm^{-2} at midday. Despite this increased radiative heating, the lower atmosphere actually cools throughout the dust event at Niamey, which illustrates the dominance of the strong advective contribution to the local

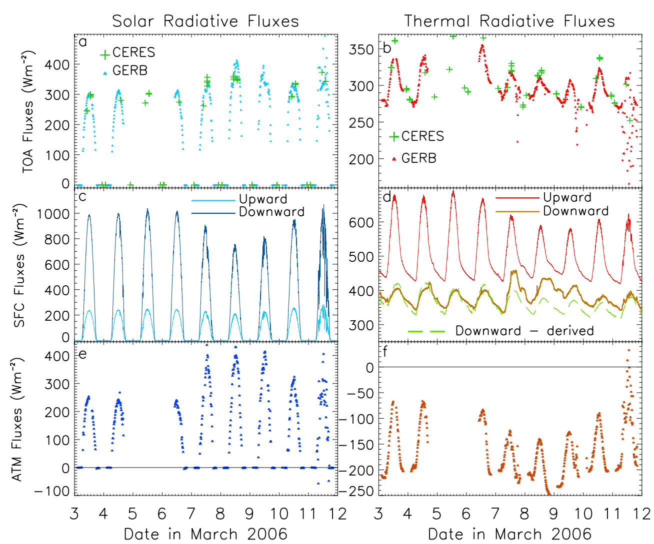

Figure 3. Solar and thermal broadband fluxes at the top of the atmosphere (TOA), at the surface (SFC), and the divergence across the atmosphere (ATM) above Niamey. (a, b) Upward fluxes at TOA from GERB and CERES. (c, d) Upward and downward surface fluxes from the radiometers at the AMF. In green; the downward thermal fluxes from the simple formula of *Prata* [1996]. (e, f) Atmospheric flux divergence (the difference between the net downward fluxes at TOA from GERB and from the AMF). The scatter on 11 March is due to cloud. See text for error estimates.

temperature from the relatively cool air flowing in from the desert.

4. Comparison With Models

[14] These radiative perturbations from the dust are much larger than the observational errors discussed earlier. Can they be reproduced by radiation models? As a first answer to this question, we ran two models [*Evans*, 1998; *Ricchiazzi et al.*, 1998] with input from the AMF measurements of the atmospheric temperature and humidity profiles, and aerosol properties retrieved from the MFRSR. We focus on solar fluxes, which show a much larger aerosol signal than the thermal fluxes. The aerosol optical depth, single scattering albedo and asymmetry parameter retrieved at the MFRSR wavelengths were interpolated to the wavelengths used in the models. A uniform aerosol layer was assumed and aerosol scattering was treated with a Henyey-Greenstein phase function. A spectral surface albedo was derived by scaling the spectral albedo of dry sand to match the AMF broadband albedo measurements. Shortwave broadband direct, diffuse, and total fluxes at the surface and at the top of the atmosphere and the resulting atmospheric divergence were calculated. Simulations were not performed for days when cloud affected the aerosol retrievals. Figure 4 compares the observed and modeled solar fluxes and the atmospheric divergence through the event, but omitting 4, 5 and 11 March when the MFRSR retrievals are affected by cloud cover.

[15] The most striking result in Figure 4 is the almost complete disappearance of the observed direct solar flux at the surface at the height of the event, due to the large aerosol optical depth (Figure 2). As a consequence, almost all the downwelling solar flux is in the diffuse component. This behavior is reproduced well by the models, with some day to day variability. The differences between the modeled and measured diffuse fluxes are consistent with some previous studies [*Halthore and Schwartz*, 2000; *Henzing et al.*, 2004] although larger than a more recent study [*Michalsky et al.*, 2006], which found agreement within 2% between modeled and diffuse fluxes in cloud-free conditions at a mid-latitude site. The aerosol loadings in the current study are a factor of 2–6 larger than in previous studies, so small errors in the specification of aerosol optical properties (e.g., single scattering albedo) or surface albedo may have large impacts on the modeled diffuse flux. While this confirms that the simulations are realistic in this respect, such skill is not entirely unexpected. The narrow-band MFRSR measurements of the spectral direct and diffuse radiances used to derive the aerosol optical properties contain similar information to that measured by the broadband radiometers, albeit in narrow spectral bands in only the visible portion of the solar spectrum. To the extent that the retrievals represent the radiatively effective properties of the aerosol and these properties can be extrapolated across the solar spectrum, we expect agreement with computed broadband fluxes. The quantitative agreement between the observed and modeled fluxes does provide an important check on the fidelity of the models. A more stringent test is to compare the upwelling fluxes at the top of the atmosphere, since these provide a completely independent test of the models. For these fluxes, the models reproduce the essential behavior, with a brightening of the planet as the aerosol arrives and a slow darkening as it dissipates. There are discrepancies; the models underestimate the upwelling fluxes before and after the event and overestimate the fluxes at the peak. When the surface and TOA fluxes are combined to estimate the atmospheric divergence, the models agree very well with the observations before and after the event, but underestimate the divergence for the peak aerosol loadings on 7, 8 and 9 March, although one model is just within two sigma of the observed estimates at all times.

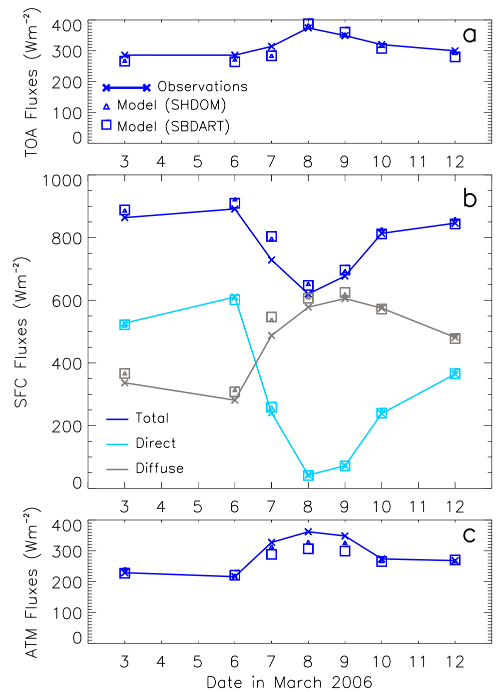

Figure 4. Observed (continuous lines) and modeled (symbols) broadband solar fluxes (Wm^{-2}), averaged from 1000–1600 local time. (a) Upward solar at the top of the atmosphere (TOA). (b) Downward solar at the surface (SFC). (c) The divergence across the atmosphere (ATM) above Niamey. See text for error estimates.

5. Discussion

[16] This paper presents the first simultaneous observations from a geostationary satellite and from a comprehensive surface site of the impact of a major Saharan dust storm on the radiation balance of the top of the atmosphere, of the surface and of the atmosphere itself. Major perturbations to the solar and thermal radiative fluxes were observed. Measurements of the atmospheric temperature and humidity profiles and retrievals of the aerosol optical properties were used as input to two radiation models, to assess their ability to simulate the impact of the dust on the solar radiation balance. The models reproduce well the behavior of the observed fluxes during the dust storm, but they underestimate slightly the solar absorption within the atmosphere.

[17] These simulations represent the first attempt to reproduce the observed fluxes and divergences during this event. Several issues need to be investigated further, including the accuracy of the aerosol retrievals in such an extreme environment and the difficult question (not

addressed here but fundamental to the ultimate goal of the RADAGAST project) of how to extend the point measurements made in Niamey to be representative of the surface fluxes over the domain covered by the satellite data. The errors introduced by the difference in scale between the surface and satellite measurements are minimised in this case study by the large spatial extent, homogeneity and thickness of the dust cloud. For more heterogeneous conditions, including clouds, this would be a more serious problem. Despite these issues, the results show that the combination of the long-term AMF measurements made in Niamey and the satellite data provide an outstanding new opportunity to further the goals of the ARM program by improving our understanding of the radiative properties of the atmosphere and by constructing test cases for evaluating and improving models.

[18] **Acknowledgments.** We thank EUMETSAT for providing limited-area subsets of the SEVIRI radiances in near real-time, the GERB Data Processing team at the Rutherford Appleton Laboratory and Imperial College in the UK and at the Royal Meteorological Institute in Brussels, Belgium, for providing preliminary data prior to public release and the staff of the ARM program who have deployed, maintained and operated the AMF in Niamey. The AMF data were provided by the U.S. Department of Energy as part of the Atmospheric Radiation Measurement Program Climate Research Facility. TPA, EIK, SAM, and JCB were supported by the Office of Biological and Environmental Research of the U.S. Department of Energy under contract DE-AC06-76RL01830 to the Pacific Northwest National Laboratory as part of the Atmospheric Radiation Measurement Program. The Pacific Northwest National Laboratory is operated by Battelle for the U.S. Department of Energy. RPA was supported by a NERC Advanced Fellowship NE/C51785X/1. We thank Jim Haywood for comments on an early version of the manuscript.

References

Ackerman, T. P., and G. M. Stokes (2003), The Atmospheric Radiation Measurement program, *Phys. Today*, *56*, 38–44.

Allan, R. P., A. Slingo, S. F. Milton, and I. Culverwell (2005), Exploitation of Geostationary Earth Radiation Budget data using simulations from a numerical weather prediction model: Methodology and data validation, *J. Geophys. Res.*, *110*, D14111, doi:10.1029/2004JD005698.

Dunion, J. P., and C. S. Velden (2004), The impact of the Saharan air layer on Atlantic tropical cyclone activity, *Bull. Am. Meteorol. Soc.*, *85*, 353–365.

Evans, K. F. (1998), The spherical harmonics discrete ordinate method for three-dimensional atmospheric radiative transfer, *J. Atmos. Sci.*, *55*, 429–446.

Halthore, R. N., and S. E. Schwartz (2000), Comparison of model-estimated and measured diffuse downward irradiance at surface in cloud-free skies, *J. Geophys. Res.*, *105*, 20,165–20,177.

Harries, J. E., et al. (2005), The Geostationary Earth Radiation Budget project, *Bull. Am. Meteorol. Soc.*, *86*, 945–960.

Harrison, L., and J. Michalsky (1994), Objective algorithms for the retrieval of optical depths from ground-based measurements, *Appl. Opt.*, *33*, 5126–5132.

Haywood, J., et al. (2003), Radiative properties and direct radiative effect of Saharan dust measured by the C-130 aircraft during SHADE: 1. Solar spectrum, *J. Geophys. Res.*, *108*(D18), 8577, doi:10.1029/2002JD002687.

Haywood, J. M., R. P. Allan, I. Culverwell, A. Slingo, S. Milton, J. Edwards, and N. Clerbaux (2005), Can desert dust explain the outgoing longwave radiation anomaly over the Sahara during July 2003?, *J. Geophys. Res.*, *110*, D05105, doi:10.1029/2004JD005232.

Henzing, J. S., et al. (2004), Effect of aerosols on the downward shortwave irradiances at the surface: Measurements versus calculations with MODTRAN4.1, *J. Geophys. Res.*, *109*, D14204, doi:10.1029/2003JD004142.

Kassianov, E. I., J. C. Barnard, and T. P. Ackerman (2005), Retrieval of aerosol microphysical properties by using surface MFRSR data: Modeling and observations, *J. Geophys. Res.*, *110*, D09201, doi:10.1029/2004JD005337.

Kaufman, Y. J., D. Tanré, and O. Boucher (2002), A satellite view of aerosols in the climate system, *Nature*, *419*, 215–223.

Knippertz, P., and A. H. Fink (2006), Synoptic and dynamic aspects of an extreme springtime Saharan dust outbreak, *Q. J. R. Meteorol. Soc.*, *132*, 1153–1177.

Lebel, T., J.-L. Redelsperger, and C. Thorncroft (2003), African Monsoon Multidisciplinary Analysis (AMMA) Project, *GEWEX News*, *13*(4), 8–9.

Mahowald, N. M., A. Baker, G. Bergametti, N. Brooks, R. Duce, T. Jickells, N. Kubilay, J. Prospero, and I. Tegen (2005), Atmospheric global dust cycle and iron inputs to the ocean, *Global Biogeochem. Cycles*, *19*, GB4025, doi:10.1029/2004GB002402.

Michalsky, J. J., G. P. Anderson, J. Barnard, J. Delamere, C. Gueymard, S. Kato, P. Kiedron, A. McComiskey, and P. Ricchiazzi (2006), Radiative closure studies for clear skies during the Atmospheric Radiation Measurement 2003 aerosol intensive observation period, *J. Geophys. Res.*, *111*, D14S90, doi:10.1029/2005JD006341.

Miller, M. A., and A. Slingo (2006), The Atmospheric Radiation Measurement (ARM) Mobile Facility (AMF) and its first international deployment: Measuring radiative flux divergence, *Bull. Am. Meteorol. Soc.*, in press.

Ohmura, A., et al. (1998), Baseline surface radiation network (BSRN/WCRP): New precision radiometry for climate research, *Bull. Am. Meteorol. Soc.*, *79*, 2115–2136.

Pope, V. D., M. L. Gallani, P. R. Rowntree, and R. A. Stratton (2000), The impact of new physical parametrizations in the Hadley Centre climate model: HadAM3, *Clim. Dyn.*, *16*, 123–146.

Prata, A. J. (1996), A new long-wave formula for estimating downward clear-sky radiation at the surface, *Q. J. R. Meteorol. Soc.*, *122*, 1127–1151.

Prospero, J. M., and P. J. Lamb (2003), African droughts and dust transport to the Caribbean: Climate change implications, *Science*, *302*, 1024–1027.

Reda, I., T. Stoffel, and D. Myers (2003), A method to calibrate a solar pyranometer for measuring reference diffuse irradiance, *Sol. Energy*, *74*, 103–112.

Ricchiazzi, P., S. R. Yang, C. Gautier, and D. Sowle (1998), SBDART: A research and teaching software tool for plane-parallel radiative transfer in the Earth's atmosphere, *Bull. Am. Meteorol. Soc.*, *79*, 2101–2114.

Schaaf, C. B., et al. (2002), First operational BRDF, albedo nadir reflectance products from MODIS, *Remote Sens. Environ.*, *83*, 135–148.

Schmetz, J., et al. (2002), An introduction to Meteosat second generation (MSG), *Bull. Am. Meteorol. Soc.*, *83*, 977–992.

Washington, R., M. C. Todd, S. Engelstaedter, S. Mbainayel, and F. Mitchell (2006), Dust and the low-level circulation over the Bodélé Depression, Chad: Observations from BoDEx 2005, *J. Geophys. Res.*, *111*, D03201, doi:10.1029/2005JD006502.

Wielicki, B. A., B. R. Barkstrom, E. F. Harrison, R. B. Lee, G. L. Smith, and J. E. Cooper (1996), Clouds and the Earth's Radiant Energy System (CERES): An Earth Observing System experiment, *Bull. Am. Meteorol. Soc.*, *77*, 853–868.

T. P. Ackerman, J. C. Barnard, E. I. Kassianov, and S. A. McFarlane, Pacific Northwest National Laboratory, P.O. Box 999, Richland, WA 99352, USA.

R. P. Allan, G. J. Robinson, and A. Slingo, Environmental Systems Science Centre, University of Reading, Harry Pitt Building, Whiteknights, Reading RG6 6AL, UK. (as@mail.nerc-essc.ac.uk)

S. Dewitte, Royal Meteorological Institute of Belgium, 3 Avenue Circulaire, B-1180 Brussels, Belgium.

J. E. Harries and J. E. Russell, Blackett Laboratory, Imperial College, London, SW7 2BZ, UK.

M. A. Miller, Brookhaven National Laboratory, Atmospheric Science Division, Building 490D, Upton, NY 11973, USA.